Copper slag as a potential source of critical elements - A case study from Tsumeb, Namibia

S. Lohmeier[1], B.G. Lottermoser[1], T. Schirmer[2], and D. Gallhofer[3]

Affiliation:
[1] Institute of Mineral Resources Engineering, RWTH Aachen University, Wüllnerstraße 2, 52062 Aachen.
[2] Institute of Disposal Research, Department of Mineralogy, Geochemistry, Salt deposits, Clausthal University of Technology, Adolph-Roemer Straße 2A, 38678 Clausthal-Zellerfeld.
[3] Institute of Earth Sciences, University of Graz, Universitätsplatz 2/II, 8010 Graz, Austria.

Correspondence to:
S. Lohmeier

Email:
lohmeier@mre.rwth-aachen.de
stephanielohmeier2017@gmail.com

Dates:
Received: 15 Sep. 2020
Accepted: 5 Dec. 2020
Published: March 2021

How to cite:
Lohmeier, S., Lottermoser, B.G., Schirmer, T., and Gallhofer, D. 2021 Copper slag as a potential source of critical elements - A case study from Tsumeb, Namibia. Journal of the Southern African Institute of Mining and Metallurgy, vol. 121, no. 3, pp. 129–142.

DOI ID:
http://dx.doi.org/10.17159/2411-9717/1383/2021

ORCID
S. Lohmeier
https://orchid.org/0000-0003-2556-2096

B.G. Lottermoser
https://orchid.org/0000-0002-8385-3898

T. Schirmer
https://orchid.org/0000-0003-3938-5860

D. Gallhofer
https://orchid.org/0000-0003-2139-7847

Synopsis

At a time of resource consumption, it is important to study the chemical composition of mining and metallurgical wastes to prevent the dissipative loss of metals and metalloids from the mining value chain. In particular, the recovery of critical elements from wastes is an option to increase the resources of such materials that are economically significant and have an overall supply risk. In this paper we report on the chemical composition, in particular the critical element content, of granulated slag originating from historical smelting activities in the Tsumeb area, Namibia. Laboratory-based inductively coupled plasma–mass spectrometry (ICP-MS) and X-ray fluorescence (XRF) analyses as well as portable X-ray fluorescence (pXRF) demonstrate that the slags are on average enriched in base metals (Cu 0.7 wt%, Pb 2.7 wt%, Zn 4.7 wt%), trace metals and metalloids (Cd approx. 50 mg/kg, Mo approx. 910 mg/kg) as well as critical elements (As approx. 6300 mg/kg, Bi approx. 3 mg/kg, Co approx. 200 mg/kg, Ga approx. 100 mg/kg, In approx. 9 mg/kg, Sb approx. 470 mg/kg). While metals and metalloids such as As, Mo and Pb can be determined reliably using pXRF instruments, the technique has inherent limitations in evaluating the contents of certain critical elements (Ga, Sb). However, there are positive correlations between the As, Mo, and Pb contents determined by pXRF and the Ga and Sb contents obtained through ICP-MS and XRF. Thus, quantitative pXRF analysis for As, Mo, and Pb allows calculation of Ga and Sb abundances in the slags. This work demonstrates that pXRF analysers are a valuable tool to screen smelting slags for their chemical composition and to predict the likely contents of critical elements.

Keywords
base metal slag, portable XRF, critical elements, secondary resource.

Introduction

The consumption of critical elements for high-technology applications is increasing exponentially, and scenarios predict that future demand will exceed current annual worldwide production (European Commission 2010, 2017). Recent improvements in extraction and recovery technologies have the potential to render secondary materials such as copper slags important sources of critical elements (*e.g.* PGE, In, Bi) (Binnemans *et al.*, 2015).

Nonferrous slags are known to be highly heterogeneous and mineralogically diverse materials (Piatak, Parsons, and Seal II, 2015). They comprise variable amounts of glass and crystallized phases and may also contain relic ore, gangue minerals, and fluxes. The composition of slags depends on the metallurgical processes and the composition of the processed ore(s) and the fluxes used. Consequently, slags display a wide range in bulk chemical composition, with major concentrations (wt% range) of Al_2O_3, SiO_2, and Fe_2O_3, and lesser amounts of TiO_2, MnO, CaO, MgO, Na_2O, K_2O, P_2O_5, and S (Piatak, Parsons and Seal II, 2015). In addition, historical nonferrous slags are commonly characterized by elevated metal and metalloid contents as a result of inefficient metal recovery technologies, with wt% levels of Cu, Pb, and Zn (Ettler, Červinka, and Johan, 2009; Lottermoser, 2002; Vítková *et al.*, 2010). The metals are contained within the silicate glass and various slag phases, as well as within primary and weathering-induced secondary minerals, including native elements, sulphides, oxides, hydroxides, chlorides, carbonates, sulphates, arsenates, and silicates (Ettler *et al.*, 2001; Piatak, Parsons, and Seal II, 2015). In these studies, laboratory-based methods have commonly been applied for the determination of major (>1 wt%) and trace elements (<0.01 wt%) (Ettler *et al.*, 2009). In particular, inductively coupled plasma–mass spectrometry (ICP-MS) and atomic absorption or emission spectrometry (AAS/AES) have proven their merits for establishing the bulk chemical composition of these slags (Potysz et al., 2015). However, the concentrations of critical elements in slags and the application of field-portable instruments like portable X-ray fluorescence (pXRF) for such targeted analysis remain largely unexplored.

The purpose of this study is to appraise the use of combined ICP-MS, AAS, XRF, and pXRF data to establish the bulk chemistry and the presence of critical elements in granulated copper slags from the Tsumeb smelter, Namibia. The pXRF method is compared with ICP-MS and XRF techniques and the application of pXRF analysis for quantitative analysis of slag samples is validated. Hence, this case study contributes to our understanding of critical elements in slags and demonstrates that pXRF is a useful addition for the chemical characterization of pyrometallurgical wastes.

Background

Smelting site

The Tsumeb smelting complex, currently operated by Dundee Precious Metals Ltd., is located approximately 430 km north of Windhoek, the capital city of Namibia, on the northern slopes of the Otavi Mountains (Figure 1). Smelting in the area goes back to 1907, when the German Otavi Minen-und Eisenbahn-Gesellschaft constructed two lead-copper blast furnaces to smelt local dolomitic ore (Mapani *et al.*, 2014). The present smelter complex was constructed in the early 1960s by Tsumeb Corporation Limited to process largely sulphidic Cu-Pb ore from the Tsumeb mine, and later also ores from Kombat (Kramer and Hultman, 1973) and Khusib Springs (Melcher, 2003). The site originally featured an integrated copper and lead section (with refinery) and smaller plants that intermittently produced cadmium metal, arsenic trioxide, and germanium (Acid Plant Database, 2020; Dundee Precious Metals Tsumeb, 2020; Mapani *et al.*, 2014, and references therein). During the early 1980s, a slag mill was built to reprocess old copper reverbatory slags, which were milled and subsequently treated by flotation. The resulting concentrate was then processed in the smelters to extract Cu and Pb. In 1986, sodium antimonite was produced (Mapani *et al.*, 2014, and references therein). Between 1980 and 1996, the reverbatory furnaces used fuel oil, and the smelting charge was pelletized with pulverized coal, as well as quartz, chert, and lime as fluxes (Ettler *et al.*, 2009; Mapani *et al.*, 2014). Since the flooding of the De Wet Shaft and the subsequent closure of the Tsumeb mine in 1996 (Bowell and Mocke, 2018), copper ores from the Democratic Republic of Congo, Zambia, Mauritania, Botswana, Greece, Russia, and in particular from Bulgaria and South America have been processed in the refurbished Ausmelt furnace, with various fluxes and fuelled with locally produced charcoal and heavy furnace oil (Jarošítková *et al.*, 2017; Kabbash and Smith, 2016; Mapani *et al.*, 2014). The granulated slag is processed in the slag milling plant and the by-product sulphuric acid is sold to industrial consumers in Namibia (Dundee Precious Metals, 2020). Tsumeb blister copper production benefits distinctly from the considerable tolerance of the Tsumeb smelter towards arsenic and lead in copper concentrates feed (Mapani *et al.*, 2014). Resulting from the long processing history, three different types of slags can be distinguished (Ettler *et al.*, 2009). Granulated slag from the reprocessing of older slags (slag type III; Ettler *et al.*, 2009) is the subject of this study.

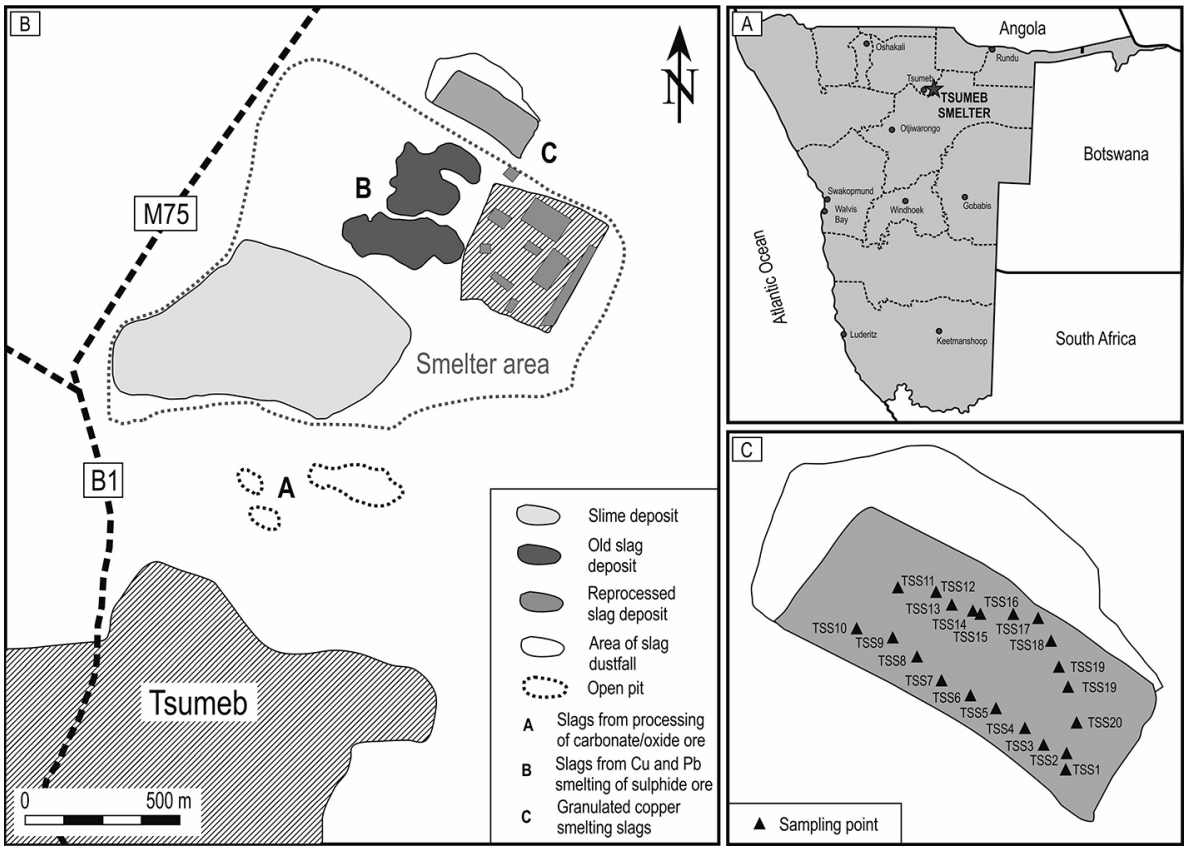

Figure 1—A: The Tsumeb smelter and the associated historical and current slags are located on the outskirts of the city of Tsumeb in the Oshikoto region of Namibia, around 500 km north of Namibia's capital city Windhoek. B: There are three different types of slags plus slimes, which can be assigned to different phases of processing activities, concomitant with changing types of processed ore (modified after Ettler *et al.*, 2009). C: Sampling points in the slag heap of granulated copper smelting slags

Materials and methods

Sampling

A large slag dump (approx. 40 000 m²) is located adjacent to the smelting complex and contains approximately 1.5 Mt of slag. At present, the reprocessed slags comprise granulated fragments ranging in grain size from a few millimetres in diameter to predominantly powder-size due to granulation and/or milling (Jarošítková *et al.*, 2017; Figures 1, 2, 3). During sampling in 2018, the slag heap was divided into 20 equal sectors (approximately 1 000 m²). Each sector was covered by a number of parallel traverses to obtain a representative 5 kg sample of powdered to millimetre-sized slag pieces from each sector (sample numbers TSS1–TSS20). An additional slag hand

Figure 2—Sampled surface of slag dump with Tsumeb smelter complex in the distance (photograph by B.G. Lottermoser, 2018)

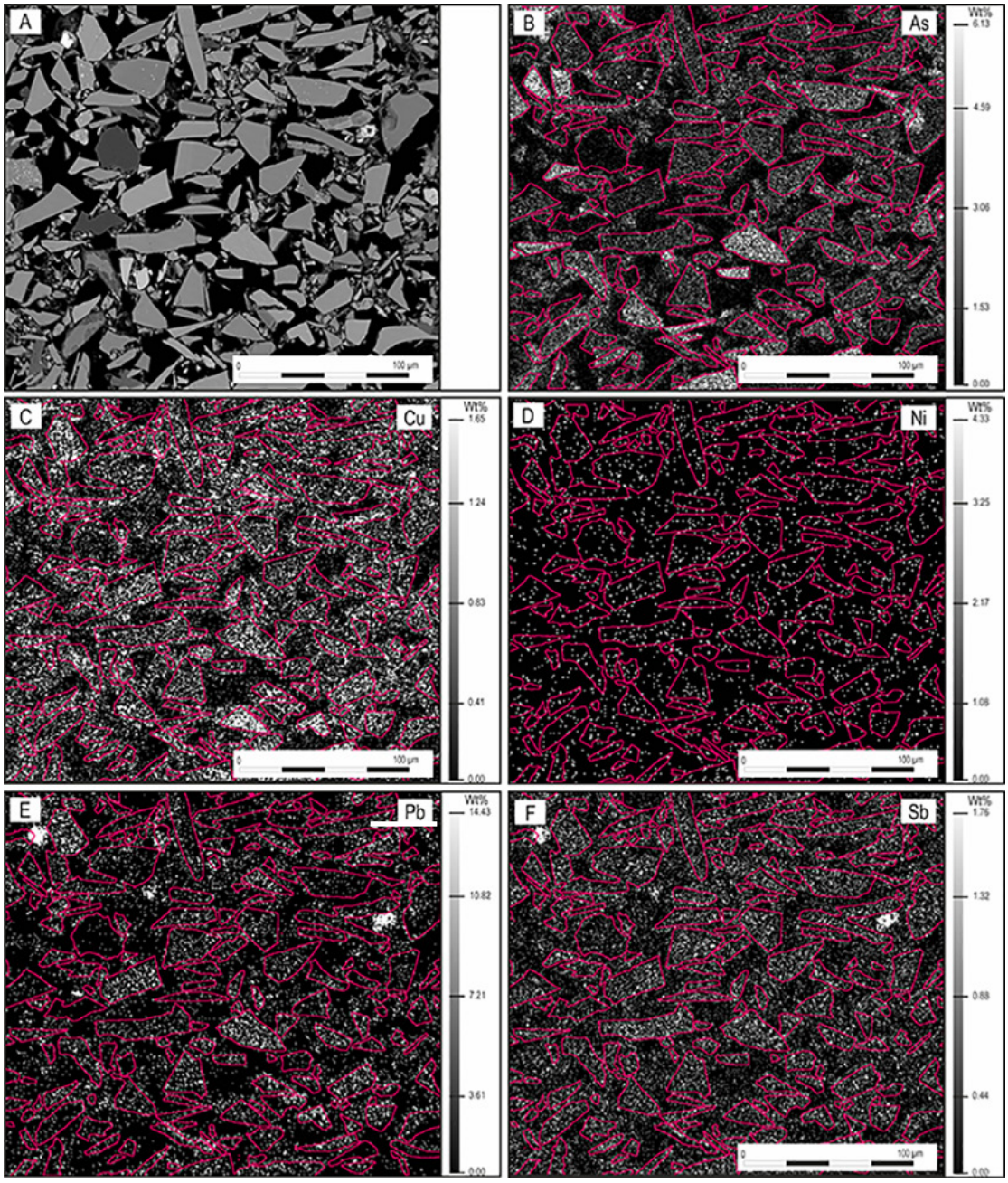

Figure 3—EMP maps of As (B), Cu (C), Ni (D), Pb (E) and Sb (F) of granulated Tsumeb slag. Red lines represent the contours of the larger crystals of the original image (A). There is a certain match of element distributions of As and Sb, as well as of Cu and Pb in the glass shards, although As is distinctly more abundant than Sb and Pb is more abundant than Cu. Analytical conditions: 15 kV, 20 nA

specimen was taken during a field sampling campaign in 2019 (sample number TSSF).

Sample processing and laboratory-based analysis

Slag samples were air-dried and homogenized. A representative aliquot was milled to analytical fineness using a tungsten-carbide swing mill in the Department of Mineral Processing at RWTH Aachen University. Milled powders were sent to SGS Bulgaria, Bor Laboratory/Serbia for conventional ICP-MS analysis for Al, As, Ba, Be, Bi, Ca, Cd, Ce, Co, Cr, Cs, Cu, Fe, Ga, Hf, In, K, La, Li, Lu, Mg, Mn, Mo, Na, Nb, Ni, P, Rb, Sb, Sc, Se, Sn, Sr, Ta, Tb, Te, Ti, Th, Tl, U, V, W, Y, Yb, and Zr after HNO_3-HF-$HClO_4$ and HCl digestion. Pb and Zn were analysed by AAS. Samples with high Cu values were re-analysed by AAS. In addition, milled powders were submitted to Australian Laboratory Services (ALS, Loughrea, Ireland) for conventional XRF analysis for major elements (Al, Ca, Fe, K, Mg, Mn, Na, P, S, Si, Ti), and minor/trace elements (As, Ba, Cl, Cr, Cu, Mo, Pb, Sb, Zn). LOI was determined by sintering at 1000°C (Table I).

XRD analyses were performed on pulps (<2 µm), using an X'Pert Pro (PANalytical) instrument with data collector and an X'Pert HighScore system equipped with a Cu-LFF (Empyrian) tube and an ADS tool at the Institute of Disposal Research (IDR) at Clausthal University of Technology (TUC). Qualitative evaluation was done using the X'Pert HighScore software from PANalytics (Figure 4).

Electron microprobe (EMP) mapping of As, Cu, Ni, Pb, and Sb was done on a slag hand-specimen mounted in epoxy resin at the IDR, TUC (Figure 3). An In-As alloy was used for As (Lα1), chalcopyrite for Cu (Kα), pentlandite for Ni (Kα), crocoite for Pb (Mα), and stibnite for Sb (Lα) calibration. EMP analyses were performed using an acceleration voltage of 15 kV and a 20 nA beam current.

Portable X-ray fluorescence spectroscopy

Chemplex sample cups were filled with milled sample powders. Prolene™ thin films were used to guarantee simple, and at the same time comparable, analytical settings. All sample cups were

Table I

Bulk rock analytical results for granulated Tsumeb slags analysed by a combination of ICP-MS, AAS. and XRF. Values of F are consistently <0.1 wt%

Analytes Method	SiO_2 [wt%] XRF	TiO_2 [wt%] ICP-MS	TiO_2 [wt%] XRF	Al_2O_3 [wt%] ICP-MS	Al_2O_3 [wt%] XRF	Fe_2O_3 [wt%] ICP-MS	Fe_2O_3 [wt%] XRF	MnO [wt%] ICP-MS	MnO [wt%] XRF	MgO [wt%] ICP-MS	MgO [wt%] XRF
TSS1	36.79	0.28	0.22	3.34	3.62	29.68	31.08	0.42	0.28	4.26	4.17
TSS2	26.43	0.25	0.20	3.12	3.62	30.47	34.19	0.49	0.34	5.24	5.52
TSS3	39.11	0.28	0.25	3.38	4.09	35.61	39.88	0.15	0.17	2.77	3.01
TSS4	38.57	0.30	0.24	3.72	4.01	34.74	35.35	0.34	0.22	3.78	3.76
TSS5	25.91	0.25	0.19	3.33	3.57	32.81	33.66	0.39	0.26	4.88	4.83
TSS6	36.76	0.30	0.22	3.74	3.80	33.84	32.21	0.51	0.31	4.86	4.37
TSS7	36.85	0.30	0.24	3.53	3.81	28.44	28.76	0.49	0.32	4.89	4.79
TSS8	34.85	0.28	0.24	3.44	3.96	29.92	32.01	0.37	0.25	4.16	4.31
TSS9	37.41	0.30	0.23	3.61	3.81	30.30	30.45	0.44	0.27	4.78	4.54
TSS10	37.29	0.32	0.24	3.91	3.92	30.62	29.42	0.49	0.30	5.22	4.75
TSS11	38.05	0.28	0.23	3.68	3.92	30.20	29.23	0.47	0.29	4.46	4.27
TSS12	36.74	0.30	0.25	3.74	4.27	33.20	34.74	0.35	0.24	3.68	3.81
TSS13	30.12	0.28	0.21	3.84	3.93	34.67	33.55	0.47	0.29	4.64	4.35
TSS14	36.67	0.30	0.23	3.72	3.89	37.80	36.73	0.36	0.22	3.85	3.62
TSS15	38.39	0.32	0.25	3.91	4.11	41.00	39.66	0.18	0.19	3.35	3.21
TSS16	38.06	0.30	0.25	3.80	4.00	39.97	39.11	0.18	0.20	3.20	3.15
TSS17	35.60	0.33	0.27	4.23	4.43	35.26	34.53	0.39	0.25	4.33	4.15
TSS18	31.08	0.35	0.27	4.93	4.85	34.91	33.04	0.45	0.28	4.91	4.37
TSS19	28.70	0.25	0.20	3.55	3.60	33.51	35.04	0.44	0.26	4.46	4.30
TSS20	23.42	0.25	0.16	3.19	3.03	35.06	34.59	0.56	0.31	5.82	5.17
TSSF	-	0.25	-	4.48	-	23.78	-	0.30	-	3.88	-

Analytes Method	CaO [wt%] ICP-MS	CaO [wt%] XRF	Na_2O [wt%] ICP-MS	Na_2O [wt%] XRF	K_2O [wt%] ICP-MS	K_2O [wt%] XRF	P_2O_5 [wt%] ICP-MS	P_2O_5 [wt%] XRF	SO_3 [wt%] XRF	Cl [mg/kg] XRF	LOI [wt%]
TSS1	15.07	11.25	1.08	1.20	0.40	0.38	0.34	0.33	0.54	60	2.71
TSS2	>20	17.50	0.94	0.15	0.48	0.50	0.23	0.22	2.00	80	3.81
TSS3	10.75	8.88	0.70	0.83	0.41	0.43	0.23	0.23	1.50	<50	4.02
TSS4	14.19	10.30	0.90	1.00	0.42	0.41	0.27	0.26	0.84	<50	3.22
TSS5	>20	16.55	1.08	1.24	0.43	0.41	0.25	0.24	2.83	70	4.07
TSS6	17.29	11.80	1.08	1.10	0.39	0.34	0.37	0.33	0.44	<50	2.56
TSS7	18.65	13.20	1.20	1.28	0.39	0.35	0.41	0.41	0.31	60	2.28
TSS8	16.92	12.70	1.00	1.16	0.41	0.42	0.32	0.34	1.07	50	2.07
TSS9	18.72	13.20	1.13	1.14	0.40	0.37	0.46	0.45	0.60	50	2.14
TSS10	20.16	13.60	1.35	1.33	0.43	0.37	0.48	0.45	0.61	50	2.09
TSS11	19.83	13.85	0.90	0.95	0.45	0.40	0.46	0.45	0.46	60	1.92
TSS12	14.82	11.00	0.88	1.00	0.46	0.46	0.27	0.28	1.08	<50	2.69
TSS13	>20	16.10	0.88	0.93	0.53	0.49	0.25	0.24	1.78	60	3.16
TSS14	14.34	10.00	0.93	0.96	0.46	0.42	0.27	0.27	1.01	50	3.46
TSS15	12.98	9.06	0.92	0.93	0.49	0.45	0.27	0.26	1.28	50	3.78
TSS16	12.89	9.43	0.81	0.87	0.51	0.48	0.25	0.26	1.28	<50	3.88
TSS17	15.42	10.80	1.27	1.32	0.53	0.51	0.27	0.27	1.20	<50	2.98
TSS18	19.48	13.20	1.39	1.42	0.71	0.63	0.27	0.24	1.62	100	2.81
TSS19	>20	14.45	1.08	1.10	0.48	0.43	0.23	0.23	2.22	90	3.15
TSS20	>20	15.20	1.00	0.93	0.54	0.46	0.21	0.19	1.38	180	3.69
TSSF	12.63	-	0.93	-	0.46	-	0.37	-	-	-	-

Table I (continued)

Bulk rock analytical results for granulated Tsumeb slags analysed by a combination of ICP-MS, AAS. and XRF. Values of F are constantly <0.1 wt%

Analytes Method	As [mg/kg] ICP-MS	As [mg/kg] XRF	Ba [mg/kg] ICP-MS	Ba [mg/kg] XRF	Be [mg/kg] ICP-MS	Bi [mg/kg] ICP-MS	Cd [mg/kg] ICP-MS	Ce [mg/kg] ICP-MS	Co [mg/kg] ICP-MS	Cr [mg/kg] ICP-MS	Cr [mg/kg] XRF
TSS1	8640	8900	1373	1523	0.6	2.10	45	70	239	380	821
TSS2	2383	2200	>10000	6359	1.2	2.91	36	55	155	152	342
TSS3	4336	4600	1450	1791	0.6	0.93	14	65	117	351	889
TSS4	5554	5200	1478	1702	0.8	2.59	42	61	235	402	821
TSS5	2094	1900	7676	4747	1.1	1.94	28	55	216	235	547
TSS6	9469	9200	1494	1612	0.5	3.18	97	71	220	447	889
TSS7	>10000	11200	1309	1523	0.9	1.14	94	69	214	406	889
TSS8	6756	7100	4456	2598	0.7	9.68	49	67	186	308	753
TSS9	9296	9500	1498	1791	0.5	4.69	107	75	189	430	1026
TSS10	9508	9500	1695	1881	1.0	4.10	52	90	188	371	821
TSS11	7454	8000	2825	2060	0.8	2.55	91	77	204	431	1026
TSS12	5169	5500	4380	2508	0.7	5.87	62	73	193	372	821
TSS13	2767	2400	8320	4568	1.2	1.91	29	61	216	305	684
TSS14	5205	5200	1701	2060	0.7	1.62	39	67	216	371	821
TSS15	4894	4800	1522	1881	0.7	2.94	18	81	132	316	684
TSS16	3434	3200	4518	2508	0.7	1.34	26	72	154	292	616
TSS17	6647	6700	4831	2598	1.0	2.62	50	76	255	313	753
TSS18	4110	3600	6720	3583	1.8	2.11	41	80	235	282	684
TSS19	3337	3000	9210	4479	1.6	2.06	26	53	248	279	547
TSS20	5488	4700	>10000	5822	1.5	4.92	69	49	249	175	342
TSSF	7528	–	928	–	0.8	1.39	60	173	131	330	-

Analytes Method	Cs [mg/kg] ICP-MS	Cu [mg/kg] ICP-MS	Cu [mg/kg] AAS	Cu [mg/kg] XRF	Ga [mg/kg] ICP-MS	Hf [mg/kg] ICP-MS	In [mg/kg] ICP-MS	La [mg/kg] ICP-MS	Li [mg/kg] ICP-MS	Lu [mg(kg] ICP-MS	Mo [mg/kg] ICP-MS	Mo [mg/kg] XRF
TSS1	0.56	7800	–	7220	170	2.21	6.65	28	21	0.42	1225	1120
TSS2	1.04	6681	–	6140	53	2.69	6.45	27	26	0.24	752	730
TSS3	0.73	6587	–	5920	63	2.07	9.13	26	18	0.32	478	490
TSS4	0.76	6512	–	5770	85	2.00	12	25	23	0.28	675	580
TSS5	1.11	6921	–	6550	64	2.29	5.18	26	26	0.22	875	870
TSS6	0.50	7856	–	7760	171	2.30	9.88	29	20	0.36	1107	1000
TSS7	0.46	8180	–	8630	194	2.32	8.07	28	24	0.44	1365	1280
TSS8	0.68	7012	–	6510	123	2.47	8.01	29	19	0.39	1074	1020
TSS9	0.34	8135	–	7690	148	2.50	8.02	31	21	0.40	1186	1120
TSS10	0.64	6609	–	6280	190	2.33	7.38	36	28	0.51	1465	1360
TSS11	0.58	7436	–	7690	108	2.33	8.02	32	21	0.45	993	930
TSS12	0.78	6860	–	6570	80	2.41	9.05	29	19	0.38	734	710
TSS13	1.06	4986	–	4690	62	2.43	9.51	28	23	0.30	734	730
TSS14	0.67	6369	–	5770	81	2.53	11	29	19	0.35	697	680
TSS15	0.69	6262	–	5740	72	2.52	9.40	31	21	0.42	566	540
TSS16	0.69	5362	–	5300	47	2.94	9.10	31	19	0.37	535	450
TSS17	0.90	7120	–	6490	104	2.91	9.28	34	23	0.38	1014	920
TSS18	1.14	6262	–	5580	90	3.38	8.21	37	27	0.42	978	980
TSS19	1.15	7455	–	7120	65	2.34	7.32	25	26	0.27	940	870
TSS20	1.13	>10000	15400	14250	54	2.46	12	24	31	0.23	867	620
TSSF	1.24	7200	-	-	127	2.34	6.22	103	24	0.49	997	-

Analytes Method	Nb [mg/kg] ICP-MS	Ni [mg/kg] ICP-MS	Pb [wt%] AAS	Pb [wt%] XRF	Rb [wt%] ICP-MS	Sb [mg/kg] ICP-MS	Sb [mg/kg] XRF	Sc [mg/kg] ICP-MS	Se [mg/kg] ICP-MS	Sn [mg/kg] ICP-MS	Sr [mg/kg] ICP-MS	Ta [mg/kg] ICP-MS
TSS1	7.1	140	3.03	2.76	16	723	710	3.7	<2	63	285	2.68
TSS2	6.0	52	2.46	2.25	17	317	340	3.7	22	48	442	1.72
TSS3	3.6	58	1.61	1.37	17	318	380	3.9	3	39	224	0.90
TSS4	5.7	123	2.21	1.88	17	604	600	4.0	3	70	296	2.42
TSS5	6.0	46	2.06	1.85	16	215	270	4.0	23	445	459	1.29
TSS6	7.6	151	3.33	3.12	13	822	800	4.1	<2	123	284	2.20
TSS7	8.0	137	3.27	3.02	14	777	810	4.0	<2	122	275	2.88
TSS8	7.5	87	2.38	2.22	15	555	580	4.0	4	84	313	1.24
TSS9	4.4	117	3.04	2.72	13	569	730	4.0	6	98	296	0.67
TSS10	11	98	2.56	2.28	16	660	680	4.3	3	97	359	1.93
TSS11	2.5	140	3.07	2.84	15	414	740	4.0	6	96	301	0.20
TSS12	6.0	93	2.09	1.98	17	503	540	4.2	5	61	327	2.00
TSS13	6.0	58	1.70	1.51	17	265	270	4.5	10	64	429	1.66
TSS14	3.1	111	2.17	1.94	16	304	530	4.2	4	53	296	0.39
TSS15	4.9	75	1.93	1.72	18	301	410	4.3	4	43	243	0.51
TSS16	6.4	64	1.55	1.39	18	301	310	4.3	<2	39	276	1.85
TSS17	7.4	105	2.54	2.33	19	541	580	5.0	8	83	327	2.22
TSS18	8.4	70	2.50	2.24	23	305	430	6.2	12	80	372	2.86
TSS19	4.5	67	2.68	2.58	17	259	350	4.3	20	53	395	1.25
TSS20	5.2	128	7.40	5.76	19	637	600	6.3	30	97	424	1.12
TSSF	9.4	94	2.85	-	17	527	-	4.2	7	97	318	0.46

Table I (continued)

Bulk rock analytical results for granulated Tsumeb slags analysed by a combination of ICP-MS, AAS. and XRF. Values of F are constantly <0.1 wt%

Analytes Method	Tb [mg/kg] ICP-MS	Te [mg/kg] ICP-MS	Th [mg/kg] ICP-MS	Tl [mg/kg] ICP-MS	U [mg/kg] ICP-MS	V [mg/kg] ICP-MS	W [mg/kg] ICP-MS	Y [mg/kg] ICP-MS	Yb [mg/kg] ICP-MS	Zn [wt%] AAS	Zn [wt%] XRF	Zr [mg/kg] ICP-MS
TSS1	0.84	0.52	18	0.94	40	231	191	32	2.8	3.97	4.06	77
TSS2	0.52	1.34	9.7	0.37	13	127	97	16	1.6	7.36	7.43	90
TSS3	0.74	0.11	7.4	0.54	22	81	85	23	2.2	2.11	2.07	80
TSS4	0.70	0.69	8.5	0.68	24	107	113	25	2.0	2.95	2.83	86
TSS5	0.50	0.72	7.7	0.37	16	96	89	18	1.5	8.89	9.04	80
TSS6	0.84	0.79	14	0.90	45	177	158	32	2.7	3.87	4.06	84
TSS7	0.94	0.38	16	0.80	46	229	200	37	3.1	3.98	4.12	87
TSS8	0.79	3.72	16	1.15	33	128	125	29	2.7	4.31	4.54	84
TSS9	0.99	1.18	21	1.13	43	146	127	36	2.8	3.48	3.45	80
TSS10	1.05	1.16	37	0.88	52	204	176	43	3.3	3.65	3.63	87
TSS11	0.95	0.69	12	1.40	59	122	59	38	3.2	3.66	3.42	83
TSS12	0.82	1.93	10	1.15	30	105	110	27	2.6	3.32	3.50	88
TSS13	0.65	0.71	9.0	0.50	19	86	96	22	2.0	5.88	6.12	94
TSS14	0.77	0.46	10	0.92	30	108	47	27	2.6	3.07	3.14	89
TSS15	0.82	0.43	9.2	0.77	29	95	54	30	2.8	2.43	2.47	91
TSS16	0.81	0.44	11	0.86	30	82	78	28	2.6	2.64	2.83	93
TSS17	0.78	0.64	16	0.84	33	106	151	26	2.4	4.71	4.85	105
TSS18	0.80	0.44	14	0.93	27	104	151	27	2.5	6.64	7.25	123
TSS19	0.62	0.56	8.6	0.53	20	88	120	19	1.9	7.81	8.19	86
TSS20	0.51	1.19	8.7	0.22	14	138	85	15	1.4	9.25	7.92	87
TSSF	0.94	0.51	33	2.23	34	118	94	30	3.0	4.30	-	78

Table II

Analytical results by pXRF for granulated Tsumeb slags. Values of Nb and Se <LOD (lower analytical detection limit)

Analytes	As [wt%]		Cu [wt%]		Mo [wt%]		Pb [wt%]		Sb [wt%]		Sn [wt%]		Zn [wt%]	
		±		±		±		±		±		±		±
TSS1	1.04	0.02	0.840	0.012	0.116	0.002	3.07	0.05	0.080	0.003	0.119	0.001	4.26	0.06
TSS2	0.295	0.011	0.769	0.020	0.073	0.001	2.15	0.05	0.033	0.002	0.117	0.000	7.44	0.07
TSS3	0.543	0.011	0.746	0.007	0.050	0.000	1.48	0.01	0.045	0.001	0.116	0.001	2.15	0.01
TSS4	0.620	0.005	0.683	0.006	0.063	0.001	2.06	0.02	0.067	0.003	0.120	0.001	2.91	0.03
TSS5	0.285	0.012	0.763	0.018	0.081	0.001	1.64	0.05	0.021	0.001	0.117	0.001	8.54	0.08
TSS6	1.01	0.02	0.841	0.018	0.092	0.003	3.33	0.09	0.082	0.003	0.125	0.002	4.07	0.09
TSS7	1.26	0.02	0.869	0.010	0.127	0.002	3.25	0.02	0.082	0.002	0.126	0.001	4.17	0.03
TSS8	0.849	0.015	0.782	0.010	0.107	0.002	2.36	0.03	0.063	0.002	0.122	0.001	4.45	0.04
TSS9	1.10	0.02	0.877	0.010	0.112	0.001	2.98	0.02	0.080	0.001	0.124	0.001	3.59	0.03
TSS10	1.03	0.01	0.690	0.012	0.130	0.002	2.41	0.02	0.067	0.002	0.122	0.001	3.70	0.03
TSS11	0.889	0.012	0.787	0.008	0.094	0.001	3.06	0.02	0.073	0.002	0.123	0.001	3.50	0.02
TSS12	0.640	0.004	0.763	0.005	0.071	0.001	2.16	0.02	0.058	0.002	0.118	0.001	3.58	0.02
TSS13	0.363	0.004	0.561	0.008	0.069	0.001	1.60	0.02	0.030	0.001	0.119	0.001	5.65	0.07
TSS14	0.662	0.007	0.731	0.024	0.069	0.001	2.16	0.04	0.059	0.002	0.118	0.001	2.95	0.05
TSS15	0.575	0.008	0.710	0.005	0.053	0.001	1.89	0.02	0.048	0.001	0.116	0.000	2.50	0.01
TSS16	0.406	0.009	0.597	0.012	0.051	0.001	1.47	0.02	0.034	0.002	0.116	0.000	2.49	0.02
TSS17	0.799	0.009	0.767	0.014	0.094	0.000	2.48	0.02	0.061	0.001	0.122	0.001	4.81	0.04
TSS18	0.485	0.010	0.677	0.002	0.088	0.001	2.40	0.01	0.032	0.001	0.120	0.001	6.74	0.03
TSS19	0.381	0.010	0.778	0.013	0.081	0.001	2.35	0.03	0.031	0.002	0.117	0.000	7.60	0.03
TSS20	0.779	0.018	1.82	0.04	0.068	0.001	5.74	0.11	0.051	0.003	0.121	0.001	7.50	0.09
TSSF	0.873	0.014	0.749	0.005	0.098	0.001	2.76	0.03	0.059	0.002	0.122	0.000	2.72	0.03

backfilled with stuffing fibre. Analysis was carried out using a Niton XL3t 900 hand-held XRF instrument connected to a radiation protection chamber at the IDR (TUC). The analyser is equipped with a 50 kV Ag target X-ray tube. Analyses were done in 'environmental mode – minerals with Cu/Zn', with a total measurement time of 100 seconds (Table II). Analyses were repeated five times. To test reproducibility and homogeneity two sample cups were prepared for each pulp; the results were almost identical. The instrument was calibrated using the following certified reference materials (CRMs): (i) OREAS 24b, 24c, 36, 37, 112, 131b, 132b, 133b, 134b, 160, 623, 932 of the OREAS pXRF Zn-Pb-Ag sulphide kit; (ii) RTS-3a and MP-1b CRMs of the CANMET Mining and Mineral Sciences Laboratories Canada, and (iii) SRM 2780 of the National Institute of Standards and Technology. Calibration factors, slope, and intercept, were obtained using the provided CorrectCalc software program of the Niton device. To monitor the drift of the instrument and to assure quality control, a set of six CRMs (OREAS 36, 131b, 132b, 133b, 134b, 623) was analysed three times at the start and at the end of every measuring day plus once after every sample (plus duplicate).

For calibration of the pXRF device, regression analysis was done using the aforementioned CRMs. The quality of the linear relationship between a CRM and a pXRF value is expressed

by the coefficient of determination (R^2), which is at the best 1.00. Very good R^2 values were obtained for TiO_2, MnO, CaO, K_2O, As, Ba, Cd, Cu, Mo, Pb, Rb, Sn and Zn (R^2 = 0.99) and for SiO_2, Fe_2O_3, S, Sb, Sr and Zr (R^2 = 0.96–0.98), when filtered for outliers. However, R^2 is low for Al_2O_3 (R^2 = 0.53), and only acceptable for MgO (R^2 = 0.86). Root mean square errors (RMSEs) are largely below unity, with the exception of SiO_2, Al_2O_3, and Fe_2O_3 (Table III).

Precision (*i.e.* the degree to which repeated measurements under unchanged conditions show the same result) and accuracy (*i.e.* proximity of measurement results to the true value) are important parameters to evaluate the quality of chemical analyses. Precision of pXRF values can be assessed via the percentage relative standard deviation (RSD), and accuracy via the relative difference (%RD), using the criteria after Jenner (1996) and Piercy and Devine (2014). Most major elements, metals, and metalloids show on average excellent (RSD 0–3%) to good (RSD 7–10%) precision, with the exception of MgO, Cd, and Rb (RSD >10%). Considering average values, As, Ba, Cu, Mo, Pb, Sn, and Zn show excellent precision (RSD 0–3%) and Sb very good precision (RSD 7–10%).

The average accuracy of pXRF data, compared to ICP-MS data and XRF data, is variable. Elements/oxides like SiO_2, TiO_2, Fe_2O_3, Cd, Cu, Mo, Pb, Sr, and Zn show an acceptable accuracy (%RD ≤20) compared to the ICP-MS and XRF values. An acceptable accuracy is also evident for MnO, CaO, Ba, and Sb compared to the XRF data, but accuracy is only within the 23–36%RD range compared to ICP-MS results. The average accuracy of As is close to 20%RD. Accuracy for Al_2O_3 is poor, as well as for MgO, Rb, and in particular Sn.

Results and discussion

Slag mineralogy

Granulated slags from Tsumeb are largely composed of X-ray amorphous substances, in particular vitreous materials, which cannot be distinguished by XRD. This feature is clearly reflected in all XRD patterns by the lack of clearly defined X-ray peaks (Figure 4). Only (synthetic) augite and quartz could be identified in most slag samples. In addition, an uncommon spinel with Cu-Zn-Al compounds is present, as well as unknown Mg-Al oxide, Mg-Fe oxide, and Pb oxide phases. The 'quartz' proportion can

Table III

Calibration factors and CRMs used for calibration. Range of precision, expressed as RSD and accuracy, expressed as %RD, for pXRF data. $\%RD_{ICP-MS}$ values refer to ICP-MS data, $\%RD_{XRF}$ values refer to XRF data. Av. |%RD| is the average absolute value of the percentage relative difference

Analytes	CRMs	R^2	RSD [%]	Av. RSD [%]	$\%RD_{ICP-MS}$	av $\|\%RD_{ICP-MS}\|$	$\%RD_{XRF}$	av $\|\%RD_{XRF}\|$
SiO_2	OREAS 24b, 24c, 131b, 132b, 133b, 134b, 160, 623, 923, RTS-3a	0.98	0.43 - 2.09	1.04			(-)15 - 2.23	4.33
TiO_2	OREAS 24b, 24c, 131b, 132b, 133b, 623, 932, MP-1b, RTS-3a, SRM 2780	0.99	3.83 - 14	7.83	(-)33 - 2.35	13	2.64 - 24	11
Al_2O_3	OREAS 24b, 24c, 131b, 132b, 133b, 134b, 160, 623, 932, MP-1b, RTS-3a, SRM 2780	0.53	0.70 - 3.41	1.93	53 - 122	93	56 - 115	82
Fe_2O_3	OREAS 24b, 24c, 36, 37, 121, 131b, 132b, 133b, 134b, 160, 623, 932, RTS-3a, SRM 2780	0.98	0.17 - 1.85	0.58	1.42 - 27	12	2.80 - 15	11
MnO	OREAS 24b, 24c, 36, 131b, 132b, 133b, 134b, 623, 932, MP-1b, RTS-3a, SRM 2780	0.99	1.66 - 6.90	3.68	(-)53 - 7.75	36	(-)15 - (-)1.50	7.85
MgO	OREAS 24b, 131b, 132b, 160, 932, MP-1b, RTS-3a, SRM 2780	0.86	8.41 - 43	22	44 - 136	76	47 - 140	80
CaO	OREAS 24b, 24c, 131b, 132b, 133b, 134b, 160, 623, 932, RTS-3a, SRM 2780	0.99	0.45 - 2.51	1.15	(-)39 - (-)17	30	(-)13 - 2.07	3.86
K_2O	OREAS 24b, 24c, 131b, 132b, 133b, 134b, 623, MP-1b, RTS-3a	0.99	1.95 - 8.29	3.97	0.79 - 42	24	19 - 44	32
SO_3	OREAS 131b, 132b, 133b, 36, 37, 623, 932, MP-1b, RTS-3a, SRM 2780	0.98	2.83 - 21	8.31				
As	OREAS 24b, 24c, 36, 37, 112, 131b, 132b, 133b, 623, 932, MP-1b, RTS-3a, SRM 2780	0.99	0.64 - 4.32	1.79	6.41 - 42	22	8.48 - 66	25
Ba	OREAS 24c, 131b, 132b, 133b, 134b, RTS-3a	0.99	0.49 - 4.65	1.84	(-)58 - 27	36	(-)16 - 11	7.51
Cd	OREAS 112, 131b, 132b, 133b, 134b, 623, 932, MP-1b	0.99	0.00 - 27	15	(-)100 - 8.17	19		
Cu	OREAS 36, 37, 112, 131b, 132b, 133b, 134b, 623, 932, MP-1b, RTS-3a, SRM 2780	0.99	0.37 - 3.23	1.54	4.34 - 15	9.86	0.74 - 27	17
Mo	OREAS 623, MP-1b, RTS-3a, SRM 2780	0.99	0.48 - 2.81	1.28	(-)21 - 5.02	7.39	(-)10 - 12	4.47
Pb	OREAS 36, 37, 131b, 132b, 133b, 134b, 623, MP-1b, SRM 2780	0.99	0.25 - 2.85	1.25	(-)20 - 3.19	4.93	(-)11 - 11	7.73
Rb	OREAS 24b, 24c, 131b, 132b,	0.99	0.00 - 24	15	41 - 188	104		
Sb	OREAS 112, 131b, 132b, 133b, 134b, 623, SRM 2780, 623, 932, RTS-3a, SRM 2780	0.96	1.12 - 6.78	3.53	(-)19 - 94	23	(-)26 - 17	10
Sn	OREAS 24b, 24c, 131b, 132b, 133b, 134b, 623, 932, MP-1b	1.00	0.38 - 1.34	0.70	916 - 2886	1751		
Sr	OREAS 24b, 24c, 131b, 132b, 623, 932, RTS- 3a, SRM 2780	0.98	0.00 - 3.12	2.02	(-)16 - 6.25	5.24		
Zn	OREAS 24b, 24c, 36, 37, 112, 131b, 132b, 133b, 134b, 623, 932,MP-1b RTS-3a, SRM 2780	0.99 0.99	0.40 - 2.09	0.91	(-)19 - 7.69	4.37	(-)12 - 4.87	3.94
Zr	OREAS 24b, 24c, 131b, 132b, 133b, 623, MP-1b, SRM 2740	0.96	0.00 - 29	9.51	(-)65 - (-)10	32		

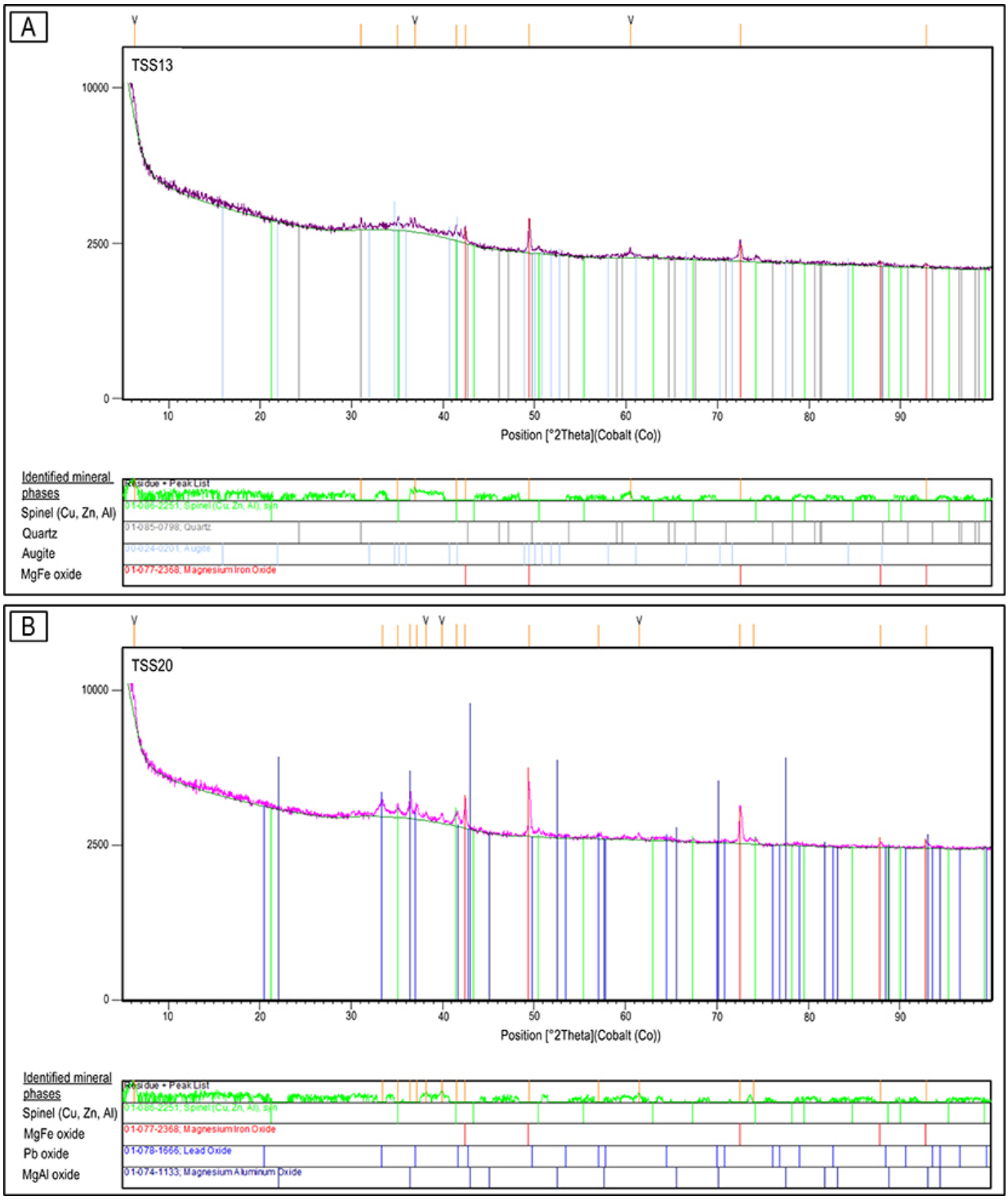

Sample	Identified substances					
	Augite (Ca, Mg, Fe) (Mg, Fe) Si_2O_6	Quartz (SiO_2)	CuZnAlspinel	MgAl oxide	MgFe oxide	Pb oxide
TSS2			X		X	
TSS5			X	X	X	
TSS6	X	X	X			
TSS7	X	X	X			
TSS9	X	X	X		X	
TSS10	X	X	X			
TSS13	X	X	X		X	
TSS20			X	X	X	X

Figure 4—XRD results for Tsumeb slag. A, B: Slag is largely composed of amorphous substances, as reflected by a very low number of depicted peaks. Only quartz and augite could be identified in almost all samples. In addition, an uncommon spinel with CuZnAl-compounds is present, as well as synthetic MgAl oxides, MgFe oxides, and Pb oxides. Almost all peaks could be assigned to a mineral, although some might be obscured in the background signal

probably be ascribed to the high-temperature, low-pressure SiO_2 compound tridymite and/or cristobalite (Figure 5). No sulphide minerals, intermetallic compounds, pure metals, or arsenates (*cf.* Ettler *et al.*, 2009) could be detected in the sampled materials.

Element mapping of As, Cu, Ni, Pb, and Sb (sample TSSF) reveals a largely very heterogeneous distribution of these elements within granulated slag powder (Figure 3) as well as within slag particles. Moreover, imaging gives clear evidence for predominance of glassy fragments in quenched milled slag. Sulphides and oxides are rare. There is a certain match between element distribution maps of As and Sb, as well as of Cu and Pb, but the distinctly greater abundance of As over Sb and Pb over Cu is obvious.

Slag geochemistry

The chemical composition of the slag samples is reported in Table I. The slags are largely composed of SiO_2 (23.42–39.11 wt%; av. 34.34 wt%), $Fe_2O_{3\ TOT}$ (28.76–39.88 wt%; av. 33.86 wt%), and CaO (8.88–17.50 wt%; av. 12.60 wt%), as well as minor Al_2O_3 (3.03–4.85 wt%; av. 3.91 wt%) and MgO (3.01–5.52 wt%; av. 4.22 wt%) as is typical for base metal slags (Figure 5). P_2O_5 and S contents are comparatively low at 0.19–0.45 wt% (av. 0.30 wt%) and 0.12–1.13 wt % (Ø 0.48), respectively. However, the slags are significantly enriched in metals and metalloids: Pb (1.55–7.40 wt%; av. 2.68 wt%), Zn (2.11–9.25 wt%; av. 4.70 wt%), Cu (4 986–15 400 mg/kg; av. 7 290 mg/kg), As (2 094–11 200 mg/kg; av. 5 607 mg/kg), Ba (1 373–6 359 mg/kg; av. 3 692 mg/kg), and Mo (478–1 465 mg/kg; av. 913 mg/kg). Likewise, high contents of >100 mg/kg are shown by Cr (152–447 mg/kg; av. 331 mg/kg), Co (117–255 mg/kg; av. 203 mg/kg), Ga (47–194 mg/kg; av. 101 mg/kg), Sb (215–822 mg/kg; av. 470 mg/kg), Sn (39–123 mg/kg; av. 73 mg/kg), Sr (224–459 mg/kg; av. 331 mg/kg), and V (81–231 mg/kg; av. 128 mg/kg). Several of these elements (As, Cr, Co, Ga, Sb, V) are considered as critical elements according to the USGS (2018). The bulk chemical composition of the granulated slags generally agrees with that documented by Ettler *et al.* (2009) and Jarošítková *et al.* (2017). Lower As and S as well as high Cd and Sb values detected in this study are likely due to higher sample numbers (Ettler *et al.*, 2009: n = 2; this study: n = 20).

Compared to average crustal abundances, the granulated slag is highly enriched in As [approx. 2 530 ×], Pb, [approx. 2 450 ×], Sb [approx. 2 350 ×], and Mo [approx. 1 140 ×]. Zn [approx. 650 ×], Cd [approx. 635 ×], Cu [270 ×], Te [approx. 180 ×], In [approx. 170 ×], and W [approx. 115 ×] also are distinctly enriched; however, W values have to be interpreted with caution as a tungsten-carbide mill was used for milling. Moreover, a notable enrichment is shown by Se [64 ×], Sn [43 ×], U [24 ×], Bi [17 ×], S [12 ×], Ba [12 ×], Co [8 ×], and Ga [6 × (Figure 6). The major elements Fe, Mn [4 ×], Ca and P [3 ×] are slightly enriched, as well as Cr, Th, Ta, Ni, Ce, and Tl [2 ×]. La, Y, Li, Tb, Yb, Lu, Sr, Mg, V, Nb, Hf, Zr, and Si have the same abundance as in average bulk continental crust. Be, Ti, Cs, Rb, Na, K, Al, and Sc are slightly depleted. The important critical elements As, Sb, Te, and In are among the most enriched elements in Tsumeb granulated slag. In addition, although less enriched, are the four critical elements Sn, U, Bi, Ga, and Co.

Prediction of geochemical composition from pXRF data

XRF and ICP-MS analysis are well-established techniques for determining the composition of geological materials and metallurgical wastes (*e.g.* Potysz *et al.*, 2015). Such instruments used for elemental analysis must be operated in a controlled laboratory environment. Progress in XRF instrumentation has opened the way to measurement of materials in the field by means of portable XRF analysis. Portable XRF can screen for multiple elements simultaneously in a variety of materials, using one device with minimal sample preparation. However, many critical elements are only poorly determined in materials by the energy-dispersive pXRF technology (Gallhofer and Lottermoser 2018). Comparison of laboratory-generated XRF and ICP-MS data with pXRF data reveals specific element trends and may allow predictions of likely chemical compositions (Figure 7).

The chemical composition of slag samples analysed by pXRF is reported in Table II. To compare pXRF with ICP-MS/AAS and XRF data, linear regression functions were calculated for pXRF – ICP-MS/AAS and pXRF – XRF data-sets, which reveal very good correlations ($R^2 \geq 0.90$) for As, Ba, Cd, Mo, P, Pb, Si, Sn, Sr, and Zn (Figure 7). Good correlations ($R^2 \geq 0.80$) are shown by Ca and Mn. Cu shows distinctly better correlations for the pXRF – ICP-

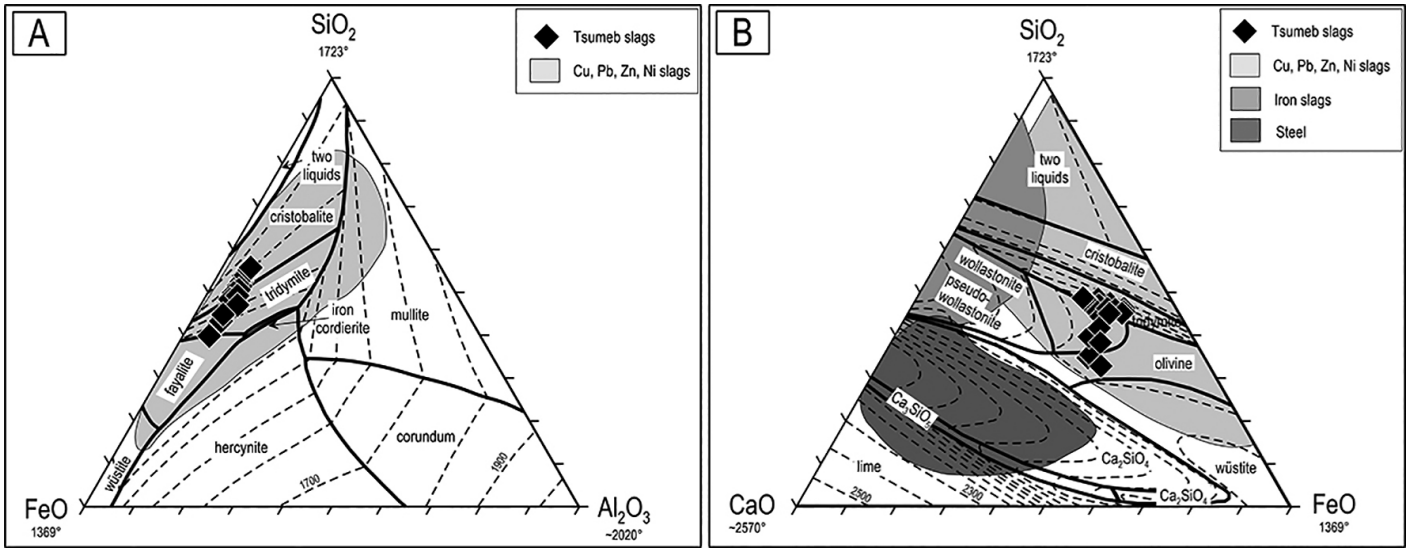

Figure 5—Bulk chemical composition of slags in Al_2O_3-SiO_2-FeO (A) and FeO-SiO_2-CaO (B) ternary diagrams. Tsumeb slag samples plot well within the field of base metal slags of Piatek, Parsons, and Seal II (2015). Diagram is based on XRF data [wt%]. Isotherms are in °C

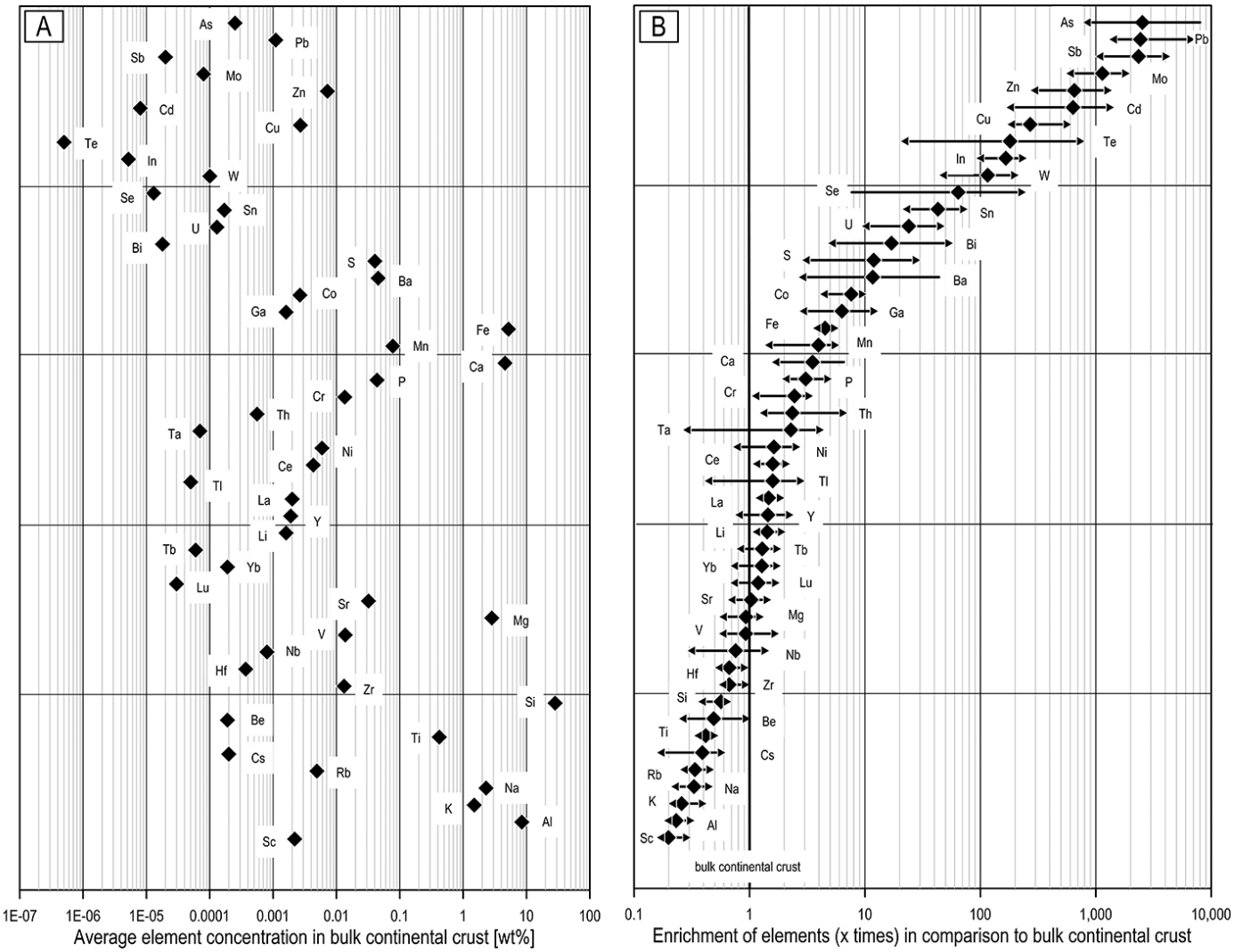

Figure 6—A: Average concentration of selected elements in bulk continental crust. B: Enrichment of selected elements in comparison to bulk continental crust based on ICP-MS data for granulated Tsumeb slags. For Si and S, XRF data was used, for Cu combined ICP-MS and AAS data, and for Pb AAS data. Elements are arranged by increasing enrichment of average values. There is a clear enrichment of As, Pb, Sb, Mo, Zn, Cd, Cu, Te, and In (>100 ×) as well as a certain enrichment of Se, Sn, U, Bi, Ba, Co, and Ga (> 5 ×). W is likewise enriched, but the values have to be interpreted with caution as a tungsten-carbide mill was used. Arrows reflect the concentration range of each element. If elements have values below/above the analytical detection limit (no arrow tip) the lower element range was set to half the lower analytical detection limit and the upper element range was set to the double the upper analytical detection limit. All values below analytical detection limits are considered with half detection limit and all values above the analytical detection limits are considered with the double detection limit. Element concentrations in bulk continental crust are taken from Rudnick and Gao (2014) and Wedepohl (1969)

MS/AAS values than for the pXRF – XRF data-sets ($R_{ICP\text{-}MS/AAS\text{-}pXRF}$ = 0.94; $R_{XRF\text{-}pXRF}$ = 0.81), but for Sb the opposite is the case ($R_{ICP\text{-}MS/AAS\text{-}pXRF}$ = 0.73; $R_{XRF\text{-}pXRF}$ = 0.92; Figure 7). Correlation of ICP-MS and XRF data is good for most elements ($R^2 \geq 0.80$), and for major elements and Sb within an acceptable range ($R^2 \geq 0.70$).

Analysis of critical elements using pXRF is notoriously difficult. In the studied slags, pXRF provides precise and accurate data for only As. Other critical elements (*e.g.* Ga, Sb, Sn) can be detected; however, accuracy is either poor or concentrations are close to the detection limit. Cobalt is difficult to analyse by pXRF, in particular if Fe is present (Sieber and Pella, 1986), due to X-ray peak overlap (Gallhofer and Lottermoser, 2018), although concentrations are in the 100–200 mg/kg range.

Calculation of correlation coefficients for element pairs from the ICP-MS and pXRF data-sets reveals clear positive correlations of Ga, Sb, and Sn (analysed by ICP-MS) with As (analysed by pXRF), as well as a less certain correlation of Mo and As. Current commercial pXRF detectors are not capable of analysing Ga routinely. Only a few detectors can analyse for Ga if concentrations are well above 100 mg/kg (Williams-Thorpe, 2008), and if the sample matrix allows Ga detection (Lemière, 2018). For the Tsumeb slags, considering that Ga concentrations correlate with the As and Mo concentrations, Ga contents can be indirectly determined by pXRF analysis of As and Mo. pXRF analyses of both As and Mo are of excellent precision, and accuracy is acceptable for As (RSD = 1.79; $\%RD_{ICP\text{-}MS}$ = 22; $\%RD_{XRF}$ = 25; averages) for both pXRF – ICP-MS and pXRF – XRF data-sets and is good for Mo (RSD = 1.28; $RD_{ICP\text{-}MS}$ = 7.39; $\%RD_{XRF}$ = 4.47; averages; Figure 8). Hence, the following linear regressions allow calculation of Ga concentrations:

$$Ga_{conc}\,[\%] = 53.82 \times As_{conc,pXRF}\,[\%] + 0.16 \quad [1]$$

$$Ga_{conc}\,[\%] = 4.48 \times Mo_{conc,pXRF}\,[\%] + 0.04 \quad [2]$$

Antimony is another critical element enriched in the Tsumeb slag, although a certain portion has already been extracted. As

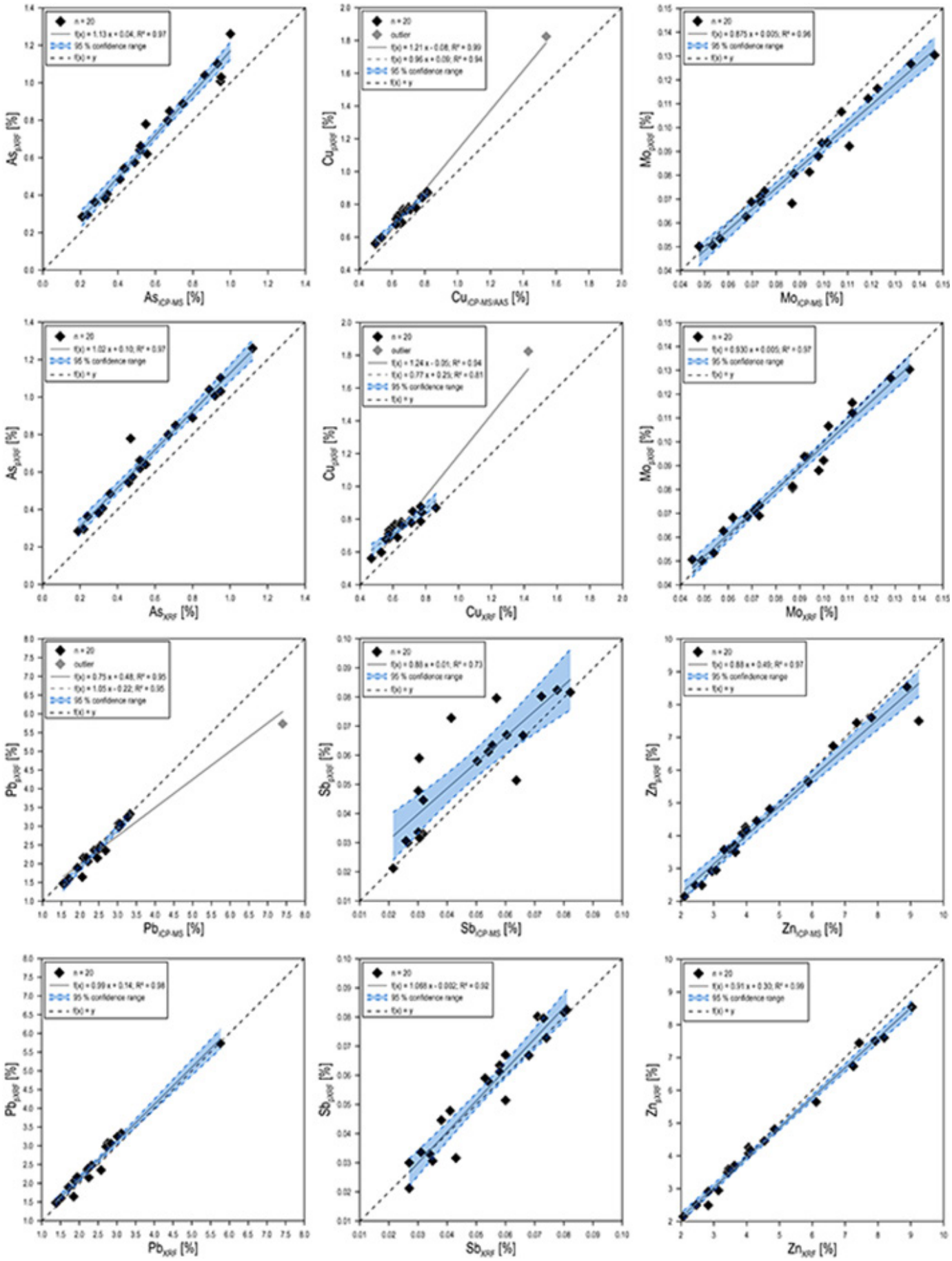

Figure 7—X-Y plots of pXRF and ICP-MS/AAS data as well as of pXRF and XRF data showing good to acceptable correlations for As, Cu, Mo, Pb, Sb, and Zn

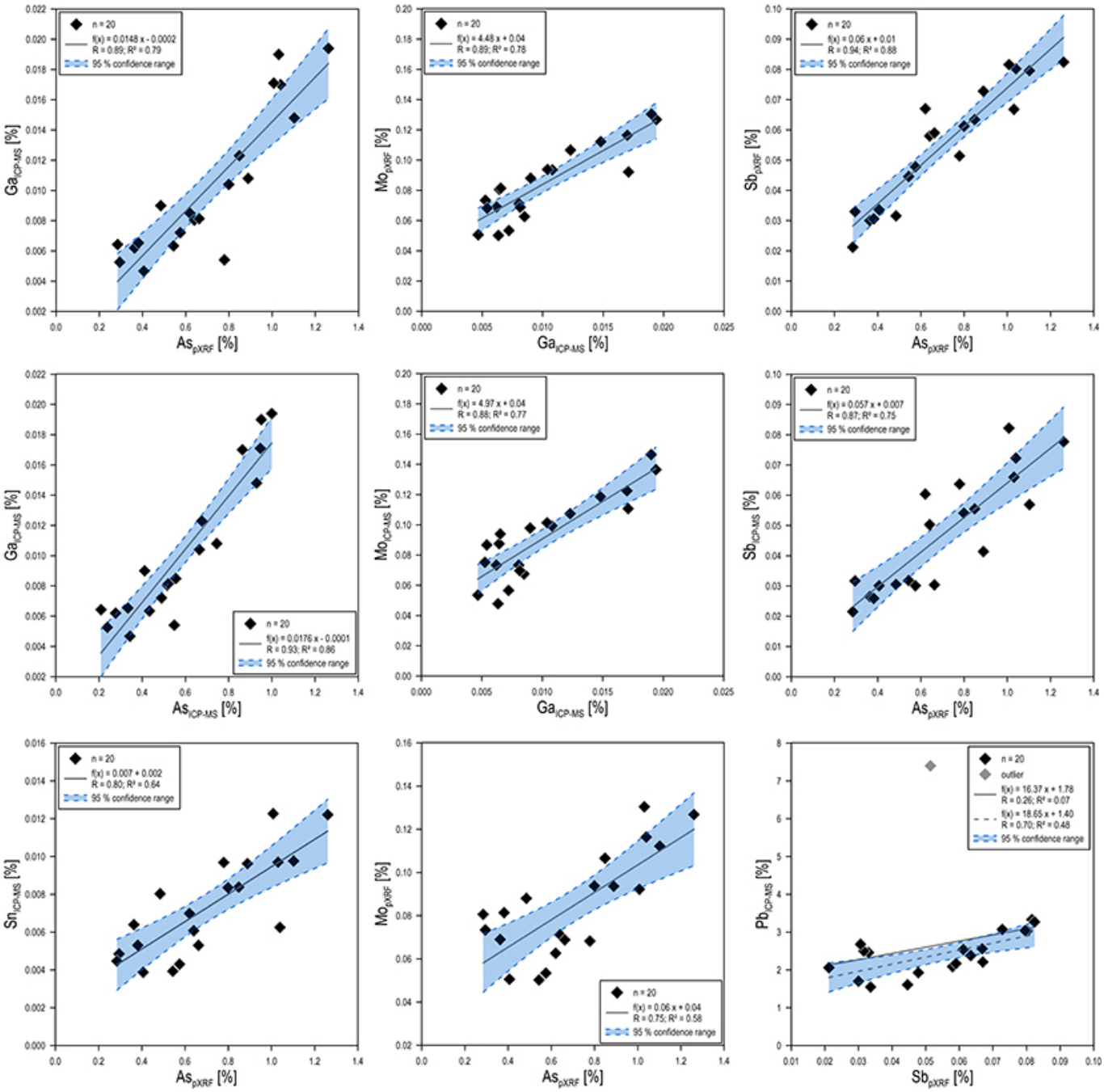

Figure 8—X-Y plots of selected elements. There is good correlation between As_{pXRF} and Ga_{ICP-MS}, As_{ICP-MS} and Ga_{ICP-MS}, Mo_{pXRF} – Ga_{ICP-MS} as well as between Mo_{ICP-MS} and Ga_{ICP-MS}, allowing the indirect, quantitative determination of Ga contents by pXRF analysis of As and/or Mo. Sb concentrations can be verified by pXRF analysis of As and Pb. Moreover, As correlates with Ga and Sb and shows a correlation with Sn and Mo

direct analysis by pXRF of Sb is acceptable, but not of good precision (RSD = 3.53; $\%RD_{ICP-MS}$ = 23; $\%RD_{XRF}$ = 10), indirect verification of pXRF-derived Sb data is recommended using Pb pXRF-derived data (Bero *et al.*, 1993). The following linear formula allows the indirect calculation of Sb contents using Pb values:

$$Sb_{conc}\,[\%] = 22.98 \times Pb_{conc,pXRF}\,[\%] + 1.27 \quad [3]$$

In addition, Sb contents can be verified from As:

$$Sb_{conc}\,[\%] = 13.12 \times As_{conc,pXRF}\,[\%] + 0.08 \quad [4]$$

Thus, a direct analysis of the critical element As enriched in Tsumeb granulated slag using low-cost on-site pXRF analysis is possible. In addition, indirect analysis of Ga and Sb is feasible, using As and Mo or Pb and As pXRF-derived data, respectively.

Reprocessing potential of Tsumeb slags

Slag compositions are influenced by the metallurgical process used and the composition of smelted ores and fluxes. At the Tsumeb smelter, ores of the Tsumeb deposit as well as other deposits close by in the Otavi Mountain Land were originally processed, which are well-known for their metal and metalloid enrichment (*i.e.* Pb, Cu, Zn, Ag, As, Sb, Cd, Co, Ge, Ga, Au, Fe, Hg, Mo, Ni, Sn, W and V) (Bowell, 2014; Frimmel, Deane and Chadwick, 1996; Melcher, 2003; Melcher, Oberthür and Rammlmair, 2006; Pirajno and Joubert, 1993).

Overall, approximately 30 Mt ore at 10% Pb, 4.3% Cu, and 3.5% Zn plus significant quantities of As, Sb, Ag, Cd, and Au were extracted from the Tsumeb deposit between 1907 and 1996 (Melcher 2003). Over time, these ores and other base metal ores from mines close by, and since 1996 from several deposits overseas, were processed in the Tsumeb smelter complex, producing Pb metal, blister Cu, and Zn concentrates with by-products Ag, Au, Ge, and Cd, and intermittently As and Sb (Kramer and Hultman, 1973; Kamona *et al*., 1999; Mapani *et al*., 2014). Therefore, the studied slags do not arise from the processing and smelting of a single ore. The chemical composition of the studied slags is the result of the metallurgical treatment of diverse base metal ores and reprocessing of older slag wastes. The Tsumeb smelter is one of few smelters worldwide that is capable of processing mixed Cu-Pb ore with high As contents (Mapani *et al*., 2014), and Tsumeb sulphidic ore is known for its arsenate content (Bowell, 2014). Thus, the very high As concentration detected within the metallurgical waste is a logical consequence; although some arsenic was temporarily extracted for production of arsenic trioxide (*cf*. Acid Plant Database, 2020). In the past, poor recovery technologies for base metals, trace metals, and metalloids as well as critical elements led to the observed element enrichments.

Tsumeb slags are enriched in the critical elements As, Bi, Ga, In, Sb, Sn, Te, and U. To date, the Southern African mineral processing and smelting industry has extracted Cu, Pb, Cd, and Sb from Tsumeb slags and flotation tailings (Guest, Svoboda, and Venter, 1988; Svoboda, Guest, and Venter, 1988). In addition, the recovery of Co from slags is possible, as demonstrated by Jones *et al.* (2002). Moreover, there are numerous studies that focus on recovery of trace elements from mining and processing residues using different technical approaches to recycle high-tech elements (*e.g*. Anand, Kanta Rao, and Jena, 1980; Gbor, Ahme, and Jia, 2000; Gbor, Hoque, and Jia, 2006; Tshiongo, Mbaya, and Maweja, 2011; Tümen and Bailey, 1990; Yang *et al*., 2010).

The Tsumeb copper slag is an under-exploited residue, from which metals, metalloids, and critical elements may be derived, *e.g*. Sn (Mapani *et al*., 2014). Successful recovery of raw materials from the existing waste would require reprocessing and adjustments to the existing metallurgical processes that would allow critical element extraction. The additional benefit of such waste valorization practices would be the prevention of metalliferous drainage and dust dispersion from the slag dump in the long term (Dundee Precious Metals Tsumeb, 2020; Ettler *et al*., 2009; Kříbek *et al*., 2014, 2018; Mapani *et al*., 2014). For example, the amorphous glassy slag matrix exhibits a certain susceptibility to leaching during weathering (Mostafa *et al*., 2001; Tshiongo, Mbaya, and Maweja, 2011). Thus, recovery of additional metals from nonferrous slags as by-products would result in two benefits: it could yield critical raw materials and prevent the development of significant environmental impacts from waste disposal.

Conclusion

This study aimed to chemically characterize the granulated copper slag at the Tsumeb smelter site and to demonstrate its potential as source of critical raw materials. In addition, it was shown that pXRF is a useful addition to the techniques for chemical characterization of pyrometallurgical wastes. The results of this study demonstrate that

(i) Tsumeb slags are enriched in base metals (Cu, Pb, Zn), trace metals and metalloids (Ba, Cd, Mo, S, Se), and critical elements (As, Bi, Ga, In, Sb, Sn, Te, U)

(ii) The critical element As can be determined in smelting slags by pXRF at excellent precision and accuracy

(iii) Other critical elements like Ga and Sb may be determined using element proxies (As, Mo, Pb) and simple linear regression functions

(iv) pXRF can be used as an additional low-cost tool for screening the chemical composition of smelting slags.

Acknowledgements

This work was supported by the German Federal Ministry of Education and Research (BMBF) and is part of the sub-Saharan based LoCoSu project; grant number 01DG16011. We thank staff of the Institute of Disposal Research of Clausthal University of Technology (Germany) for their help with the preparation of polished thin sections and access to the microprobe. Thanks to F. Türck for his patience and support during the many long days of pXRF analysis. Thanks to the Department of Processing at the RWTH Aachen University, in particular D. Gürsel and P. Ihl, for providing access to powder preparation equipment and their never-ending patience. Thanks to Dr. R. Ellmies (Gecko Namibia) for help and patience in the field.

Authors contribution

Conceptualization: B.G.L.; sampling: B.G.L., D.G., S.L.; methodology: D.G., S.L.; validation: S.L.; formal analysis: S.L., T.S.; data curation: S.L.; writing - original draft preparation: S.L.; writing - review and editing: B.G.L., D.G., T.S.; funding acquisition: B.G.L.

References

Acid Plant Database. 2020. http://www.sulphuric-acid.com/sulphuric-acid-on-the-web/acid%20plants/Namibia-Custom-Smelter.htm [accessed 19 May 2020].

Anand, S., Kanta Rao, P., and Jena, P.K. 1980. Recovery of metal values from copper converter and smelter slags by ferric chloride leaching. *Hydrometallurgy*, vol. 5. pp. 355–365.

Bero, B.N., von Braun, M.C., Knowles, C.R., and Hammel, J.E. 1993. The use of X-ray fluorescence to detect lead contamination of carpeted surfaces. *Environment, Monitoring and Assessment*, vol. 27. pp. 17–33.

Binnemans, K., Jones, P.T., Blanpain, B., van Gerven, T., and Pontikes, Y. 2015. Towards zero-waste valorisation of rare-earth-containing industrial process residues: a critical review. *Journal of Cleaner Production*, vol. 99. pp. 17–38.

Bowell, R.J. 2014. Hydrogeochemistry of the Tsumeb deposit: Implications for arsenate mineral stability. *Reviews in Mineralogy and Geochemistry*, vol. 79. pp. 589–627.

Bowell, R.J. and Mocke, H. 2018. Minerals new to Tsumeb. *Communications of the Geological Survey of Namibia*, vol. 19. pp. 20–46.

Dundee Precious Metals Tsumeb. 2020. https://www.dundeeprecious.com/English/Operating-Regions/Current-Operations/Tsumeb/Overview/default.aspx [accessed 19 May 2020].

Ettler, V., Červinka, R., and Johan, Z. 2009. Mineralogy of medieval slags from lead and silver smelting (Bohutín, Příbram district, Czech Republic): Towards estimation of historical smelting conditions. *Archaeometry*, vol. 51, no. 6. pp. 987–1007.

Ettler, V., Johan, Z., Kříbek, B., Šebek, O., and Mihaljevič, M. 2009. Mineralogy and environmental stability of slags from the Tsumeb smelter, Namibia. *Applied Geochemistry*, vol. 24. pp. 1–15.

Ettler, V., Legendre, O., Bodénan, F., and Touray, J.-C. 2001. Primary phases and natural weathering of old lead-zinc pyrometallurgical slag from Příbram, Czech Republic. *The Canadian Mineralogist*, vol., 39. pp. 873-888.

European Commission. 2010. Critical raw materials for the EU. Report of the ad-hoc working group on defining critical raw materials. European Commission, Brussels.

European Commission. 2017. Study on the review of the list of critical raw materials – criticality assessments. European Commission, Brussels.

Frimmel, H.E., Deane, J.G., and Chadwick, P.J. 1996. Pan-African tectonism and the genesis of base metal sulfide deposits in the northern foreland of the Damara orogen, Namibia. *Society of Economic Geologists, Special Publications*, vol. 4. pp. 204–217.

Gallhofer, D. and Lottermoser, B.G. 2018. The influence of spectral interferences on critical element determination with portable X-ray fluorescence (pXRF). *Minerals*, vol. 8, no. 320. doi: 10.3390/MIN8080320

Gbor, P.K., Ahmed, I.B., and Jia, C.Q. 2000. Behaviour of Co and Ni during aqueous sulphur dioxide leaching of nickel smelter slag. *Hydrometallurgy*, vol. 57. pp. 13–22.

Gbor, P.K., Hoque, S., and Jia, C.Q. 2006. Dissolution behaviour of Fe, Co, and Ni from non-ferrous smelter slag in aqueous sulphur dioxide. *Hydrometallurgy*, vol. 81. pp. 130–141.

Guest, R.N., Svoboda, J., and Venter, W.J.C. 1988. The use of gravity and magnetic separation to recover copper and lead from Tsumeb flotation tailings. *Journal of the South African Institute of Mining and Metallurgy*, vol. 88, no. 1. pp 21–26.

Jarošíková, A., Ettler, V., Mihaljevič, M., Kříbek, B., and Mapani, B. 2017. The pH-dependent leaching behaviour of slags from various stages of a copper smelting process: environmental implications. *Journal of Environmental Management*, vol. 187. pp. 178–186.

Jenner, G.A. 1996. Trace element geochemistry of igneous rocks: geochemical nomenclature and analytical geochemistry. *Geological Association of Canada, Short Course Notes*, vol. 12. pp. 51–77.

Jones, R.T., Denton, G.M., Reynolds, Q.G., Parker, J.A.L., and van Tonder, G.J.J. 2002. Recovery of cobalt from slag in a DC arc furnace at Chambishi, Zambia. *Journal of the South African Institute of Mining and Metallurgy*, vol. 102, no. 1. pp. 5–9.

Kabbash, A. and Smith, A. 2016. Dundee's world-class acid plant demonstrates the latest in sustainable technology. *Sulfuric Acid Today*, vol. 2, no. 2. pp. 30–32.

Kamona, A.F., Lévêque, J., Friedrich, G., and Haack, U. 1999. Lead isotopes of the carbonate-hosted Kabwe, Tsumeb, and Kipushi Pb-Zn-Cu sulphide deposits in relation to Pan African orogenesis in the Damaran-Lufilian fold belt of Central Africa. *Mineralium Deposita*, vol. 34. pp. 273–283.

Kramer, R. and Hultman, T. 1973. Tsumeb – a profile of United States contribution to underdevelopment in Namibia. Corporate Information Centre of the National Council of Churches, New York.

Kříbek, B., Majer, V., Pašava, J., Knésl, I., Kamona, F., Mapani, B., Mwiya, S., Kawali, L., Kandjii, L., and Keder, J. 2014. Impact of ore processing on the environment in the Tsumeb area, Namibia. *Communications of the Geological Survey of Namibia*, vol. 15. pp. 111–116.

Kříbek, B., Šípková, A., Ettler, V., Mihaljevič, M., Majer, V., Knésl, I., Mapani, B., Penížek, V., Vaněk, A., and Sracek, O. 2018. Variability of the copper isotopic composition in soil and grass affected by mining and smelting in Tsumeb, Namibia. *Chemical Geology*, vol. 493. pp. 121–135.

Lemière, B. 2018. A review of pXRF (field portable X-ray fluorescence) applications for applied geochemistry. *Journal of Geochemical Exploration*, vol. 188. pp. 350–363.

Lottermoser, B.G. 2002. Mobilization of heavy metals from historical smelting slag dumps, north Queensland, Australia. *Mineralogical Magazine*, vol. 66, no. 4. pp. 475–490.

Mapani, B., Ellmies, R., Hahn, L., Schneider, G., Ndalulilwa, K., Leonard, R., Zeeuw, M., Mwananawa, N., Uugulu, S., Namene, E., Amaambo, W., Sibanda, F., and Mufenda, M. 2014. Contamination of agricultural products in the surrounding of the Tsumeb smelter complex. *Communications of the Geological Survey of Namibia*, vol. 15. pp. 92–110.

Melcher, F. 2003. The Otavi Mountain Land in Namibia: Tsumeb, germanium and snowball earth. *Mitteilungen der Österreichischen Geologischen Gesellschaft*, vol. 148. pp. 413–435.

Melcher, F., Oberthür, T., and Rammlmair, D. 2006. Geochemical and mineralogical distribution of germanium in the Khusib Springs Cu-Zn-Pb-Ag sulfide deposit, Otavi Mountain Land, Namibia. *Ore Geology Reviews*, vol. 28. pp. 32–56.

Mostafa, N.Y., El-Hemaly, S.A.S., Al-Wakeel, E.I., El-Korashy, S.A., and Brown, P.W. 2001. Characterization and evaluation of the hydraulic activity of water-cooled slag and air-cooled slag. *Cement and Concrete Research*, vol. 31. pp. 899–904.

Piatak, N.M., Parsons, M.B., and Seal II, R.R. 2015. Characteristics and environmental aspects of slag: a review. *Applied Geochemistry*, vol. 57. pp. 236–266.

Piercy, S.J. and Devine, M.C. 2014. Analysis of powdered reference materials and known samples with a benchtop, field portable X-ray fluorescence (pXRF) spectrometer: evaluation of performance and potential application for exploration lithogeochemistry. *Geochemistry: Exploration, Environment, Analysis*, vol. 14, no. 2. pp. 139–148.

Pirajno, F. and Joubert, B.D. 1993. An overview of carbonate-hosted mineral deposits in the Otavi Mountain Land, Namibia: implications for ore genesis. *Journal of African Earth Sciences*, vol. 16, no. 3. pp. 265–272.

Potysz, A., van Hullebusch, E.D., Kierczak, J., Grybos, M., Lens, P.N.L., and Guibaud, G. 2015. Copper metallurgical slags – current knowledge and fate: a review. *Critical Reviews in Environmental Science and Technology*, vol., 45. pp. 2424–2488.

Rudnick, R.L. and Gao, S. 2003. Composition of the continental crust. *Treatise on Geochemistry*, vol. 3. pp. 1–64.

Sieber, J.R. and Pella, P.A. 1986. Improved determination of cobalt in steel by X-ray fluorescence analysis. *X-ray Spectrometry*, vol. 15. pp. 287–288.

Svoboda, J., Guest, R.N., and Venter, W.J.C. 1988. The recovery of copper and lead minerals from Tsumeb flotation tailings by magnetic separation. *Journal of the South African Institute of Mining and Metallurgy*, vol. 88, no. 1. pp. 9–19.

Tshiongo, N., Mbaya, R.K.K., and Maweja, K. 2011. Leaching kinetics of Cu, Co, Zn, Pb and Fe from copper smelting slags cooled in different ways after tapping. *Proceedings of the VI Southern African Base Metals Conference*, Phalaborwa, 18-21 July 2011. Southern African Institute of Mining and Metallurgy, Johannesburg. pp. 463–476.

Tümen, F. and Bailey, N.T. 1990. Recovery of metal values from copper smelter slags by roasting with pyrite. *Hydrometallurgy*, vol. 25. pp. 317–328.

USGS. 2018. Draft critical mineral list – summary of methodology and background information – US Geological Survey technical input document in response to Secretarial Order no. 3359. Open-File Report 2018-1021. https://doi.org/10.3133/ofr20181021

Vítková, M., Ettler, V., Johan, Z., Kříbek, B., Šebek, O., and Mihaljevič, M. 2010. Primary and secondary phases in copper-cobalt smelting slags from the Copperbelt Province, Zambia. *Mineralogical Magazine*, vol. 74, no. 4 pp. 581–600.

Wedepohl, K.H. 1969. Handbook of Geochemistry. 1st edn. Springer, Berlin-Heidelberg.

Williams-Thorpe, O. 2008. The application of portable X-ray fluorescence analysis to archaeological lithic provenancing. *Portable X-ray Fluorescence Spectrometry – Capabilities for in situ Analysis*. Potts, P.J. and West, M. (eds.). Royal Society of Chemistry. Cambridge, UK. pp. 174–205.

Yang, Z., Rui-Lin, M., Wang-Dong, N., and Hui, W. 2010. Selective leaching of base metals from copper smelter slag. *Hydrometallurgy*, vol. 103. pp. 25–29. ◆